Sensor applications

Low-Cost Fast-Start Amplifier Architecture for AC-Coupled Measurement of Low-Frequency Signals

Aaron B. Carman* and Changzhi Li**

Department of Electrical and Computer Engineering, Texas Tech University, Lubbock, TX 79409 USA
**Graduate Student Member, IEEE*
***Fellow, IEEE*

Manuscript received 12 February 2024; revised 12 March 2024; accepted 19 March 2024. Date of publication 26 March 2024; date of current version 9 April 2024.

Abstract—As sensors become more widely deployed around humans, radar sensors have seen considerable use as a method of measuring low-frequency body motions, such as heartbeat, respiration, and gesture commands. These sensors, however, can suffer from long startup times due to the need to preserve low-frequency information. This letter presents a fast-start amplifier architecture that leverages low-cost components in a simple architecture to improve the startup time of practical sensors without impacting low-frequency response. The theory of the fast-start circuit is presented and verified through simulation to demonstrate the startup time improvement offered by the architecture. The system is then evaluated experimentally using a custom test board, with results showing an improvement in startup time compared with traditional amplifier architectures, which makes it highly useful for low-cost, low-frequency motion sensors.

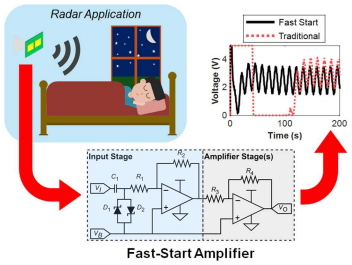

Index Terms—Sensor applications, amplifier architectures, analog fast start, baseband amplifier, fast-start sensors, low cost, passive fast start, radar.

I. INTRODUCTION

With interest in the Internet of Things (IoT), smart home technology, smart cities, and wireless health monitoring continuing to grow, microwave radar sensors have seen commensurate growth as a method of monitoring microscopic motions or target position in a noncontact fashion, allowing for integration in a greater number of complex environments [1], [2], [3]. Especially when considering the privacy aspects of dense sensor networks, microwave radar can precisely measure target metrics without needing to perform imaging, allowing for privacy to be maintained when compared with camera-based sensors [4]. Many forms of radar have been explored as potential sensors, each of which reports unique performance in various sensing tasks compared with other architectures [5]. Interferometric radar, for example, can extract target motion with micrometers of resolution, allowing for the measurement of infrastructure motion for preventative maintenance [6] or monitoring of vital signs in home healthcare technologies [7]. Oftentimes, the output of the direct-conversion receiver is quite small in amplitude, and as such must be amplified before being digitized for signal processing. In many instances, however, the dc information can be orders of magnitude larger than the ac signals of interest, requiring ac-coupled amplifiers to prevent saturation and introducing high-pass frequency behavior that can attenuate low-frequency signals of interest [8]. This can be avoided by ensuring that the cutoff frequency of the amplifier is less than the lowest frequency signal of interest but creates a new limitation in the form of long startup times. These long startup times correspond to data loss and energy waste during the startup stage when the radar output cannot be measured, both of which are counterproductive to effective sensors. DC-coupled amplifiers with adaptive dc cancellation have been proposed but require several new components that further increase system complexity and cost [9], [10], [11], preventing dense deployment of sensor networks. Simple low-cost fast-start amplifiers have been previously developed but have so far not been rigorously analyzed [12]. Software-defined techniques have also been evaluated, but again require more advanced software capabilities and introduce the potential for loop instability caused by the iterative nature of software-controlled tuning [13].

This letter proposes a low-cost fast-startup baseband amplifier that leverages two commercial diodes to achieve an optimal tradeoff between system complexity, startup time, and low-frequency amplifier performance. An example system using the proposed architecture is highlighted in Fig. 1, where the addition of the proposed fast-start architecture decreases the amplifier startup time considerably compared with traditional ac-coupled designs. The theory of the fast-start amplifier is first presented to provide an intuitive understanding of the amplifier's operation and is then confirmed via a simulation study. The results are then evaluated in an experimental setting, with the results showing that the low-cost fast-start baseband amplifier can achieve a faster startup time compared with traditional amplifiers while maintaining good low-frequency response.

II. FAST-START AMPLIFIER THEORY

In traditional ac-coupled amplifiers, dc information is removed using a coupling capacitor at the amplifier's input. In this case, the combination of input capacitance and resistance creates a high-pass response with a cutoff frequency described by (1), where R_1 and C_1, illustrated in Fig. 2, are the values of the input resistor and capacitor, respectively. Similarly, the values of R_1 and C_1 also dictate the time

Corresponding author: Aaron B. Carman. (e-mail: aaron.b.carman@ttu.edu).
Associate Editor: J. M Corres.
Digital Object Identifier 10.1109/LSENS.2024.3381918

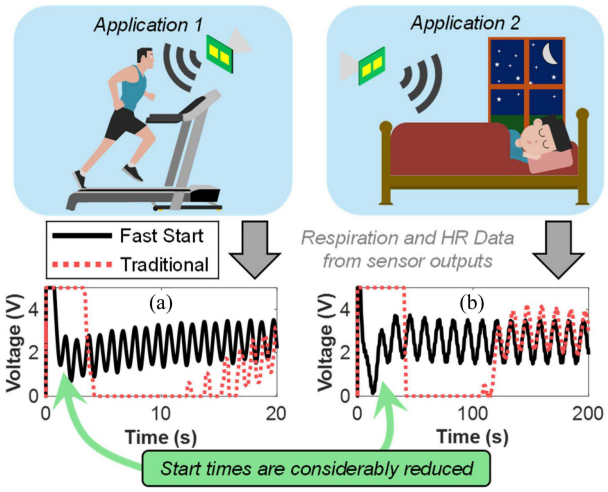

Fig. 1. Example applications leveraging the proposed fast-start amplifier. In both (a) exercise monitoring and (b) sleep studies, the startup time suffers due to the low cutoff frequency. Using the proposed fast-start amplifier, however, startup times can be shortened.

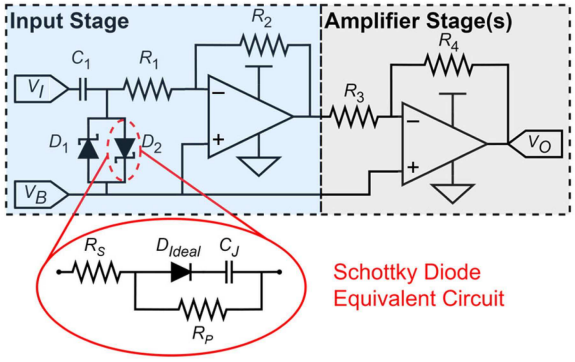

Fig. 2. Fast-start amplifier block diagram. The input stage uses two Schottky diodes to provide a low-resistance path for initial charging while allowing normal gain and frequency response after startup.

constant of the amplifier given in (2). As a result, there is a tradeoff between achieving a sufficiently low cutoff frequency and a fast startup time due to the inverse relationship between f_C and τ

$$f_C = \frac{1}{2\pi R_1 C_1} = \frac{1}{2\pi\tau} \tag{1}$$

$$\tau = R_1\, C_1. \tag{2}$$

As a result, leveraging traditional baseband amplifier designs for low-frequency signals can introduce limitations that reduce the operating efficiency of radar sensors. If a realistic case is considered, a cutoff frequency of 0.01 Hz could be used to monitor vital signs for sleep studies with little distortion. With traditional designs, however, the associated time constant would be approximately 16 s. In this case, it would take approximately 48 s for the capacitor voltage to reach 95% of its final value using capacitor charging formulas [14], which presents a major limitation to the utility of the sensor if a long time is needed before data can be gathered.

A. Amplifier Model

To model the fast-start baseband amplifier, a two-stage architecture is first considered. This architecture is illustrated in Fig. 2. The first stage is responsible for removing the dc information from the radar's output signal and accomplishing a fast start, whereas the second stage is used to provide gain to the ac-coupled signal. As was previously discussed, the long startup times associated with low-frequency baseband amplifiers are a result of the large resistances and capacitances used to reduce the lower cutoff frequency of the amplifier. As a result, when charging or discharging a large ac coupling capacitor, such as C_1, the only route for the charge to flow is through proportionally large resistances. During this time, the dc offset introduced by the capacitor is mismatched to the dc bias of the amplifier, creating an error that is amplified and saturates the output. To minimize the impact of this saturation, the input capacitor must be rapidly charged upon startup through a low-resistance path that is disabled during normal operation to ensure adequate low-frequency performance. This can be accomplished using two diodes to provide this low-resistance path when the voltage difference between the amplifier's dc bias point and the ac-coupled radar output is greater than the diode's forward voltage. It is worth noting that fast-start diodes could be used in later stages if large capacitors are present. However, since the outputs of intermediate stages oscillate around the same bias level, including fast-start diodes at intermediate stages has little impact on startup times. Furthermore, adding fast-start diodes after signal amplification can introduce nonidealities during normal operation as signal amplitude increases. Intuitively, the diodes clamp the ac-coupled input signal, preventing large dc voltage differences from being present at the capacitor's output terminal. While for large signals, this would be detrimental due to clamping and distortion; for the very small amplitude signals at the radar front end's output, the fast-start diodes only have an impact during startup. Once the capacitor voltage is within the range set by the diodes, the diodes cease conducting and have little impact on the amplifier. As a result, the effect of large dc transients can be mitigated using inexpensive components and a simple amplifier architecture. In addition, since the ac component of a radar's output is typically quite small, the effects of distortion and clamping are minimal on the final amplified signal.

B. Diode Selection

Although the presented architecture is relatively simple, selecting the diodes to provide the fast-start performance is nontrivial. Primarily, a low forward voltage is desired to maximize the fast-start performance. In other words, it would be preferred to only charge the input capacitor via an *RC* circuit for 0.35 V in the case of a Schottky diode versus 0.7 V in the case of a normal PN diode. Furthermore, the diode's parasitics can also have a tremendous impact on the performance of the amplifier. If, for example, the diode presents a large capacitance, this will alter the low-frequency performance of the amplifier and negate any benefits afforded by the diode. The impacts of reverse leakage current can also change the amplifier's frequency response if the value of R_P is comparable to the values of R_1 and R_2. As a result, a diode with a low forward voltage, small C_J, and high R_P is desired to minimize impacts after startup. While this can be accomplished using a theoretical assessment of diode characteristics, a simulation study is likely to provide a more intuitive understanding of the diode's impact on fast-start and low-frequency performance.

C. Simulation Study

To evaluate the theoretical benefits of the proposed fast-start amplifier, a SPICE simulation is used along with commercial diode models. In addition, the impacts of amplifier gain are examined to demonstrate how the proposed design adapts to meet the unique requirements of other sensors. Throughout the simulation study, the amplifier architecture in Fig. 2 is used. Intuitively, the first stage can be thought to quickly remove the dc information via the diodes and ensure that the output

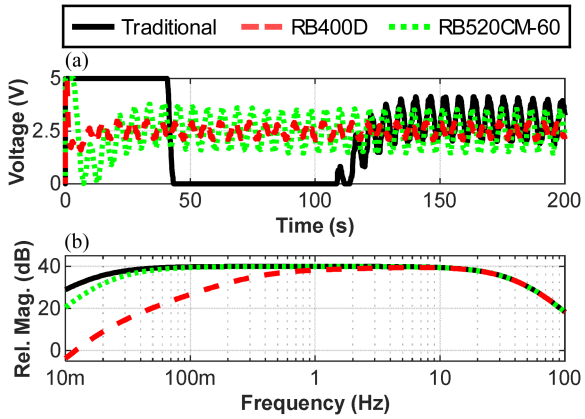

Fig. 3. (a) Time- and (b) frequency-domain simulation results. The RB520CM-60 (dotted) offers improved startup times compared with traditional design (solid) with minimal ac impact. Poor diode selection (dashed) can impact both time- and frequency-domain performances.

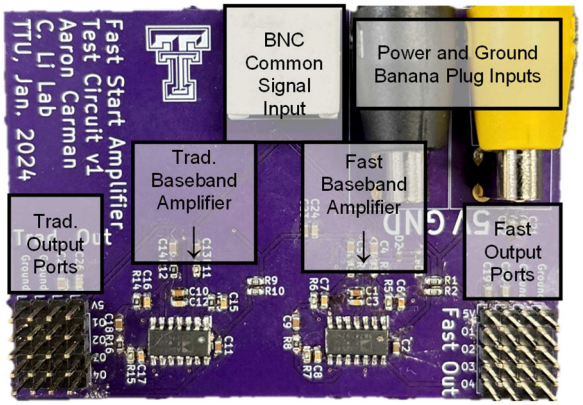

Fig. 4. Experimental circuit board and test setup. The input signal is routed to the proposed fast-start design and a traditional amplifier to evaluate the performance under matching conditions.

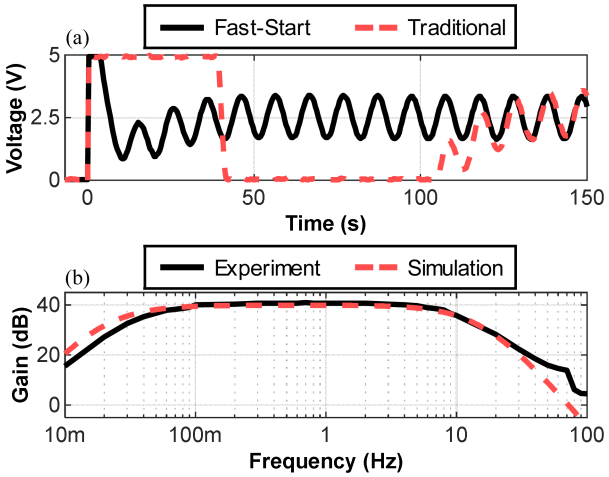

Fig. 5. Results using experimental test system. The (a) time-domain results show the improved startup time, whereas the (b) frequency-domain results show sustained good low-frequency performance.

signal is centered at the optimal point. The second stage is a typical inverting amplifier design and can be used to determine the impacts of gain on the final performance of the amplifier. It is worth noting that while R_2 and R_1 in Fig. 2 are chosen to provide unity gain in this letter, the first stage can provide gain. This, however, can have adverse impacts on practical systems due to the larger values of resistance and capacitance needed. As such, this study assumes that the first stage is always unity gain, whereas the following stages are responsible for providing gain. A total gain of 40 dB is implemented for the initial simulation study.

As a first step, a Schottky diode is selected to find an acceptable combination of capacitance, leakage current, and forward voltage to provide a faster start without adversely impacting steady-state operation. To compare the performance of diodes, a figure of merit is defined by (3), where I_R is the leakage current in nA, C_J is the junction capacitance in pF, and V_F is the forward voltage in V

$$FOM = \frac{1}{I_R C_J V_F}. \tag{3}$$

The RB520CM-60 Schottky diode was found to work well in this simulation study, providing a highly accelerated startup time without impacting the low-frequency response after startup. The associated FOM of the RB520CM-60 diode is 2.22. The simulation is also performed using the RB400D Schottky diode with an associated FOM of 3.26×10^{-4}. The startup results both with and without the discussed diodes are shown in Fig. 3(a), where the RB520CM-60 diodes show improved startup times while maintaining low-frequency gain. The associated frequency-domain results are shown in Fig. 3(b), where only a 0.013-Hz bandwidth reduction can be seen with the addition of the RB520CM-60 diodes, whereas the RB400D diodes have a much greater impact on amplifier operation in the form of a 0.512-Hz bandwidth reduction and attenuation at frequencies of interest.

III. EXPERIMENTAL RESULTS

To evaluate the performance of the proposed fast-start architecture on low-frequency sensing, an experimental system is developed. The experimental system leverages the fast-start architecture shown in Fig. 2, with the AD8544 operational amplifier providing amplification and the RB520CM-60 Schottky diode used to provide the fast-start path. Compared with Fig. 2, the gain of the amplifier is distributed across two inverting amplifier stages each with a gain of 20 dB (40 dB total), with a final unity gain buffer stage used to decouple the experimental results from the impedance of the measurement equipment. A second baseband amplifier without fast-start diodes is also implemented onboard to provide a direct comparison between fast-start and traditional amplifier performance under similar input conditions. Both amplifiers were designed to have gain fluctuations of less than 1 dB from 0.1 to 10 Hz. The test system is shown in Fig. 4.

A. Time Domain Experiments

To quantify the impact on startup time, a time domain experiment is first conducted. These experiments leverage a low-distortion function generator to create a 0.1 Hz sinusoid with 20 mV_{pp} amplitude to mimic the low-frequency output of a radar sensor. The output signal of both the fast-start and traditional baseband amplifier is recorded after startup to determine the impact on startup time. Before startup, both amplifier capacitors were allowed to discharge to simulate an unknown power-on event after a long period of no power. The results of this study are shown in Fig. 5(a). From the results, an approximately 100 s startup time reduction is observed. If a commercial radar sensor is considered [15], this startup reduction corresponds to an energy savings of over 57 J due to the ability to quickly collect meaningful data after startup.

TABLE 1. Comparison with Previous Works

Ref.	[9]	[13]	This work
Coupling	DC	DC	AC
Solution	Hardware	Software	Hardware
Integration Level	Board	IC	Board
Additional Parts[a]	15	Custom CMOS	2
Complexity	High	Medium	Low
Cost	Medium	High	Low

[a]Inferred from schematic.

As such, the system provides experimental verification of the fast-start amplifier's ability to improve startup times with little added cost and complexity.

B. Frequency Domain Experiments

To ensure that the inclusion of fast-start diodes does not impact the low-frequency ac gain of the amplifier, experiments are also conducted in the frequency domain. The amplifiers are first powered ON and allowed to settle to their normal operating point, and then, the input signal frequency is varied from 0.01 to 100 Hz in logarithmic steps. The output voltage is measured at each step to quantify the amplifier gain versus frequency. The results of this study are shown in Fig. 5(b). From the results, a modification of the low-frequency performance compared with the traditional baseband amplifier can be seen that closely follows the simulated results in Fig. 3(b). Within the frequency range of interest, however, the ac performance of the fast-start amplifier experiences little gain reduction. Table 1 provides a comparison of the proposed circuit topology with previous works, where it is seen that the proposed fast startup circuit can provide good performance improvements with a simple and low-cost ac-coupled amplifier architecture.

IV. CONCLUSION

This letter presented a low-frequency ac-coupled amplifier leveraging a passive fast-start circuit to reduce the cost and improve the performance of practical baseband amplifiers. The fast-start diodes provide a path for rapid charging of input capacitors and have little impact on circuit operation after startup. Guidelines on proper diode selection are provided to minimize the impacts on normal amplifier operation. The amplifier is analyzed theoretically and with simulation, with results being confirmed using an experimental system to directly compare the performance of traditional and fast-start amplifiers. The overall results demonstrate that the proposed architecture is a simple, low-cost solution to reduce the startup time of practical low-frequency amplifiers. Future works should focus on further analysis of the impacts of amplifier characteristics on startup performance, such as gain, cutoff frequency, or input offset voltage.

ACKNOWLEDGMENT

This work was supported by the National Science Foundation (NSF) under Grant ECCS-2028863 and Grant ECCS-2112003.

REFERENCES

[1] C. Gu and J. Lien, "A two-tone radar sensor for concurrent detection of absolute distance and relative movement for gesture sensing," *IEEE Sens. Lett.*, vol. 1, no. 3, Jun. 2017, Art. no. 3500504.
[2] J. Liu, C. Gu, Y. Zhang, and J.-F. Mao, "Analysis on a 77 GHz MIMO radar for touchless gesture sensing," *IEEE Sens. Lett.*, vol. 4, no. 5, May 2020, Art. no. 3500804.
[3] P. Vaishnav and A. Santra, "Continuous Human activity classification with unscented Kalman filter tracking using FMCW radar," *IEEE Sens. Lett.*, vol. 4, no. 5, May 2020, Art. no. 7001704.
[4] E. L. Chuma, L. L. B. Roger, G. G. de Oliveira, Y. Iano, and D. Pajuelo, "Internet of Things (IoT) privacy–protected, fall-detection system for the elderly using the radar sensors and deep learning," in *Proc. IEEE Int. Smart Cities Conf. (ISC2)*, 2020, pp. 1–4.
[5] J.-C. Chiao et al., "Applications of microwaves in medicine," *IEEE J. Microw.*, vol. 3, no. 1, pp. 134–169, Jan. 2023.
[6] D. V. Q. Rodrigues, D. Zuo, and C. Li, "Wind-induced displacement analysis for a traffic light structure based on a low-cost Doppler radar array," *IEEE Trans. Instrum. Meas.*, vol. 70, pp. 1–9, 2021.
[7] C. Gu, Y. He, and J. Zhu, "Noncontact vital sensing with a miniaturized 2.4 GHz circularly polarized Doppler radar," *IEEE Sens. Lett.*, vol. 3, no. 7, Jul. 2019, Art. no. 3501204.
[8] A. Singh, S. U. Rehman, S. Yongchareon, and P. H. J. Chong, "Multi-resident non-contact vital sign monitoring using radar: A review," *IEEE Sens. J.*, vol. 21, no. 4, pp. 4061–4084, Feb. 2021.
[9] D. Tang, J. Wang, W. Hu, Z. Peng, Y.-C. Chiang, and C. Li, "A DC-coupled high dynamic range biomedical radar sensor with fast-settling analog DC offset cancelation," *IEEE Trans. Instrum. Meas.*, vol. 68, no. 5, pp. 1441–1450, May 2019.
[10] D. Tang, J. Wang, Z. Peng, Y.-C. Chiang, and C. Li, "A DC-coupled biomedical radar sensor with analog DC offset calibration circuit," in *Proc. IEEE Int. Instrum. Meas. Technol. Conf. (I2MTC)*, 2018, pp. 1–6.
[11] Z. Peng, A. Mishra, J. R. Davis, J. A. Bridge, and C. Li, "Long-time non-contact water level measurement with a 5.8-GHz DC-coupled interferometry radar," in *Proc. IEEE Int. Instrum. Meas. Technol. Conf. (I2MTC)*, 2018, pp. 1–5.
[12] A. B. Carman and C. Li, "Passive multistatic wireless sensing based on discrete LNA/Mixer Co-optimization and fast-startup baseband amplifier," in *Proc. IEEE Topical Conf. Wirel. Sensors Sensor Netw.*, 2023, pp. 43–45.
[13] Y. Yang, C. Gu, R. Gale, J. Chen, and C. Li, "DC-coupled Doppler radar sensor with software-configured fine-tuning architectures for precise monitoring of complex motion patterns," in *Proc. IEEE Wirel. Microw. Technol. Conf.*, 2012, pp. 1–6.
[14] C. Alexander and M. Sadiku, *Fundamentals of Electric Circuits*, 6th ed., New York, NY, USA: McGraw-Hill Educ., 2017.
[15] Infineon Technologies, "BGT60UTR11AIP," Accessed: Mar. 30, 2024. [Online]. Available: https://www.infineon.com/cms/en/product/sensor/radar-sensors/radar-sensors-for-iot/60ghz-radar/bgt60utr11aip/